Supporting Information

DeCaen et al. 10.1073/pnas.0912307106

SI Text

SI Results

Structure of the NaChBac Voltage Sensor. The amino acid sequence of the S2 and S4 segments of the NaChBac voltage sensor and those of other sodium and potassium channels are illustrated in Fig. S1*A*. The 3-D structure of the NaChBac voltage sensor in resting and activated states as modeled by the Rosetta program (1) is illustrated in Fig. S1*B*.

Deactivation and Inactivation of Disulfide-Locked Channels. WT channels rapidly deactivate within 1.5 ms following a depolarizing pulse (Fig. S2*A*, left, arrow). In contrast, rapid deactivation is lost in the disulfide-locked double-cysteine mutant, and I_{Na} decays with a slow time course ($\tau \approx 320 \pm 27$ ms), comparable to inactivation of I_{Na} (Fig. S2*A*, right, arrow, compare with rate of inactivation of WT during the depolarization in Fig. S2*A*, left). Therefore, disulfide locking of E70C:R4C involves voltage-driven movement of the S4 segment to bring E70 and R4 in to close proximity, followed by disulfide locking of the voltage sensor in an activated position that induces pore opening and then inactivation (Fig. S2*B*). It is likely that inactivation of NaChBac is analogous to slow inactivation of vertebrate sodium channels because it has no structure that is analogous to the fast inactivation gate (2).

Disulfide Locking of D60C:R4C in the Presence of CuP. As illustrated in Fig. S3, exposure of D60C:R4C to the oxidizing agent CuP has no effect on sodium currents conducted by WT or single cysteine substitution mutants in response to repetitive depolarizations (Fig. S3*A*). In contrast, sodium current of the double cysteine mutant D60C:R4C is rapidly reduced by repetitive depolarizations in the presence of CuP (Fig. S3*A*). The loss of sodium current is reversed by reduction of disulfide bonds with DTT or TCEP (Fig. S3 *B* and *C*).

Mutant Cycle Analysis. We used mutant cycle analysis to assess the energy of association of these amino acid residues during activation of NaChBac channels (3, 4). The single mutations D60C and R4C shifted the $V_{1/2}$ for activation to more positive membrane potentials (Fig. S4*A*). The increases in energy required to activate these single-mutant channels is substantial (D60C, $\Delta\Delta G^\circ = 2.6$ kcal/mol; R4C, $\Delta\Delta G^\circ = 5.2$ kcal/mol; Fig. S4*C*). The double-mutant D60C:R4C activates at even more positive voltages in the absence of oxidizing agent (Fig. S4 *A* and *C*). However, this further increase in energy required for activation is less than the sum of those for the single-mutants, resulting in a coupling energy ($\Sigma\Delta G^\circ$) of −1.7 kcal/mol for the noncovalent interaction between R4C and D60C (Fig. S4 *A* and *C*). This mutant cycle analysis indicates that D60 and R4 are energetically coupled during the activation process and thus suggests that this pair may interact as counter charges in the native channel.

In contrast to R4C and D60C, the E70C single mutation shifted the $V_{1/2}$ for activation negatively, but this negative shift in the voltage dependence was accompanied by a reduction in the effective charge parameter Z ($Z = 2.3 \pm 0.1$) compared to WT ($Z = 3.8 \pm 0.1$), which together resulted in an insignificant change in the energy of activation (E70C, $\Delta\Delta G^\circ = -0.1$ kcal/mol). Pairing of mutations in E70C:R4C facilitated activation by negatively shifting $V_{1/2}$ by −36 mV relative to WT with little change in the slope of the voltage dependence (Fig. S4 *B* and *C*). Quantitative analysis of the free energies of activation of the single-mutant and double-mutant channels relative to WT yields a coupling free energy ($\Sigma\Delta G^\circ$) of −8.2 kcal/mol (Fig. S4*C*). This large coupling energy indicates that E70C and R4C interact with each other during gating. Importantly, the magnitude of the coupling energy for the noncovalent interaction of D60C with R4C (−1.7 kcal/mol) was 6.5 kcal/mol less than that for E70C:R4C channels, consistent with the energetics of formation of the covalent disulfide bond by E70C:R4C channels.

Specificity of Disulfide Locking and Energy Coupling. To examine the specificity of disulfide locking, we generated cysteine double-mutants of the S4–S5 linker residue R132 in combination with D60 and E70 (D60C:R132C and E70C:R132C) and the hydrophobic residue adjacent to R1 in combination with D60 (D60C:I114C). The positive charge at position R132 and the hydrophobic residue I114 in NaChBac are not conserved and are not hypothesized to interact with the S2 negatively charged residues during gating (Fig. S5*A*). Repetitive stimulation of E70C:R132C or D60C:R132C did not induce disulfide locking (Fig. S5*B*), and mutant cycle analysis did not reveal energy coupling for these residues (Fig. S5 *C–F*). Evidently, the S4–S5 linker residue R132 does not interact with the S2 negatively charged residues during channel activation, and the hydrophobic position I114 does not interact with the S2 extracellular negatively charged residue D60.

SI Methods

Electrophysiology. Cells were seeded onto glass coverslips and placed in perfusion chamber for experiments. Extracellular solution contained 150 mM $NaCl_2$, 1.5 mM $CaCl_2$, 1 mM $MgCl_2$, 2 mM KCl, 10 mM glucose, 10 mM Hepes, pH 7.4. The intracellular (pipet) solution contained 105 mM CsF, 10 mM EGTA, 35 mM NaCl, 4 mM Mg-ATP, 10 mM Hepes, pH 7.4. Oxidizing agents H_2O_2 or CuP, and reducing agents DTT, βME, and TCEP were added to the extracellular solution at the final concentrations as indicated and used within 20 min. For experiments using oxidizing agents and reducing agents, cells were continuously perfused with extracellular solution (2–3 mL/min). Steady-state effects for induction or reversal of disulfide locking of E70C:R4C and D60C:R4C channels were achieved after 3–5 min of exposure to reagents and were monitored by recording changes in I_{Na} during 500-ms pulses to 0 mV from a holding potential of −140 mV applied at 0.1 Hz. In experiments with E70C:R4C and D60C:R4C channels, residual linear leak and capacitance were measured with depolarizations applied to disulfide-locked and inactivated channels and subtracted offline using IGOR Pro 6.00 (Wavemetrics). The voltage dependence of activation was characterized using fits of $(V - V_{Rev})/\{1 + \exp[(V - V_{1/2})/k]\}$ to current-voltage relationships, where V_{Rev} was the extrapolated reversal potential, $V_{1/2}$ was the half activation voltage, and k was a slope factor equal to RT/ZF; Z was the apparent gating charge. Exponential decay of inactivating currents were fit with: $C + A(e^{-t/\tau})$ where A was the amplitude, τ was the time constant, and C was the baseline.

Calculation of Rate Constants for Reversal of Disulfide Locking. For calculation of rate constants, we assumed that the plateau value in βME at strongly negative potentials from Fig. 3*A* represented the amount of current available when channels were fully unlocked. Using this value for normalization, the fraction of unlocked channels at −160 mV, f, in each condition was $\beta/(\alpha +$

β). The rate of unlocking in each condition was $(\alpha + \beta) = 1/\tau$. The individual rate constants presented in Fig. 3 *C* and *D* were calculated as $\beta = f/\tau$; $\alpha = 1/\tau - \beta$.

Thermodynamic Mutant Cycle Analysis. The parameter Z was determined from fits to current-voltage relationships as described above. The amount of free energy required to shift the channel from the closed to the open state was calculated as $\Delta G^{\circ}_{C\rightarrow O}$ (kcal/mol) = $23.06ZV_{½}$, where $V_{1/2}$ was the half activation voltage in mV. The perturbation in free energy of the mutant channel relative to the wild-type was calculated as $\Delta\Delta G^{\circ} = \Delta(ZV_{½}) = 23.06[Z_{mut}V_{1/2mut} - Z_{wt}V_{1/2wt}]$. Coupling of nonadditive free energy was calculated as $\Sigma\Delta G^{\circ}_{coupled} = \Delta\Delta G^{\circ}_{Mut1:Mut2} - (\Delta\Delta G^{\circ}_{Mut1} + \Delta\Delta G^{\circ}_{Mut2})$ (4).

Homology/De Novo Modeling of the Voltage-Sensing Domain of NaChBac. The open state Kv1.2 structure was used as a template to build the activated state 2 model of the voltage-sensing domain of NaChBac (5). The activated state 1 and activated state 3 structures were modeled using the Rosetta Membrane domain assembly method and the activated state 1 state model of the voltage-sensing domain of NaChBac as a starting template and applying distance constraints between Cβ atoms of either E70 (in S2) and R4 (in S4) for activated state 1 state model or D60 (in S2) and R4 (in S4) for activated state 3 state model. Loops between the S1–S2, S2–S3, and S3–S4 segments were modeled using the Rosetta Membrane de novo method (1). The side chains in the low-resolution Rosetta method were represented by a pseudo atom, called a "centroid," the position of which was calculated for each residue as the average position of the side-chain atoms in residues of the same amino acid id entity and with φ and ψ angles in the same $10 \times 10^{\circ}$ bin and taken from known protein structures in the PDB (1). Five thousand models were generated followed by model clustering. The representative models shown were chosen from one of the top 10 cluster centers, which defined as having the lowest root mean square deviation value (between positions of Cα atoms of all residues) to all other models in a cluster. The structures in Fig. S1*A* were generated using Molscript (6) and Raster3D (7). The full atom and molecular surface representation of the voltage-sensing domain of NaChBac in Fig. 6 was generated using Chimera (8).

1. Yarov-Yarovoy V, Schonbrun J, Baker D (2006) Multipass membrane protein structure prediction using Rosetta. *Proteins* 62:1010–1025.
2. Pavlov E, et al. (2005) The pore, not cytoplasmic domains, underlies inactivation in a prokaryotic sodium channel. *Biophys J* 89:232–242.
3. Serrano L, Neira J-L, Sancho J, Fersht AR (1992) Effect of alanine versus glycine in α-helices on protein stability. *Nature* 356:453–455.
4. Yifrach O, MacKinnon R (2002) Energetics of pore opening in a voltage-gated K^+ channel. *Cell* 111:231–239.
5. Long SB, Tao X, Campbell EB, MacKinnon R (2007) Atomic structure of a voltage-dependent K^+ channel in a lipid membrane-like environment. *Nature* 450:376–382.
6. Kraulis PJ (1991) MOLSCRIPT: A program to produce both detailed and schematic plots of proteins. *J Appl Cryst* 24:946–950.
7. Merritt EA, Bacon DJ (1997) Raster3D: Photorealistic molecular graphics. *Methods Enzymol* 277:505–524.
8. Pettersen EF, et al. (2004) UCSF Chimera—A visualization system for exploratory research and analysis. *J Comput Chem* 25:1605–1612.

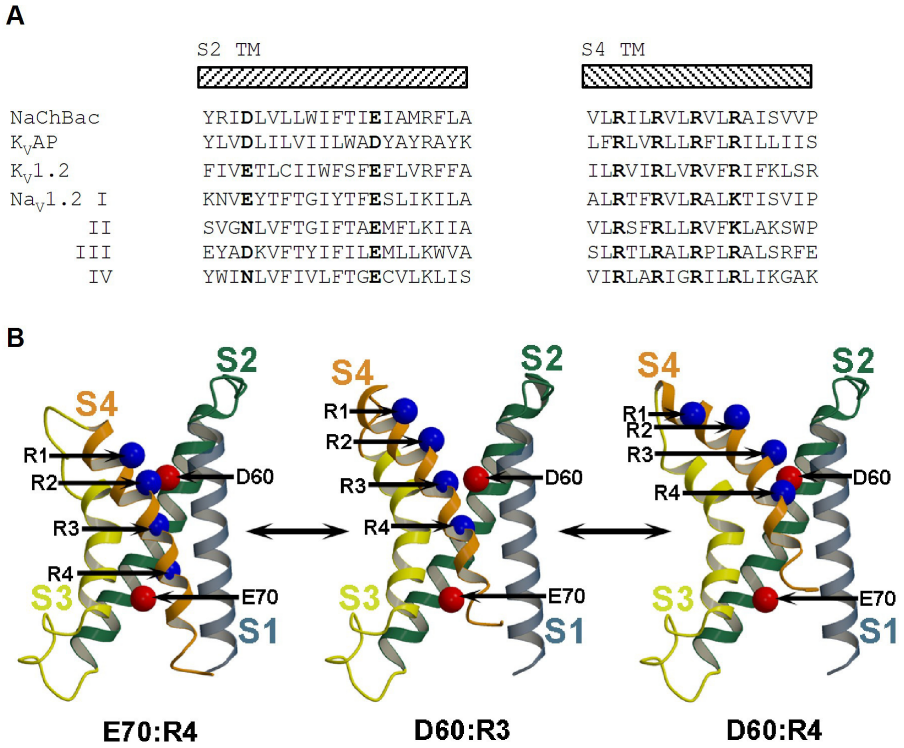

Fig. S1. Structure of the NaChBac voltage sensor. (*A*) Amino acid sequence alignment of the voltage sensors of NaChBac and other sodium and potassium channels. Conserved arginine gating charges in S4 and conserved negatively charged residues in S2 are highlighted in bold. (*B*) Rosetta models of the voltage sensors of NaChBac in resting and activated states.

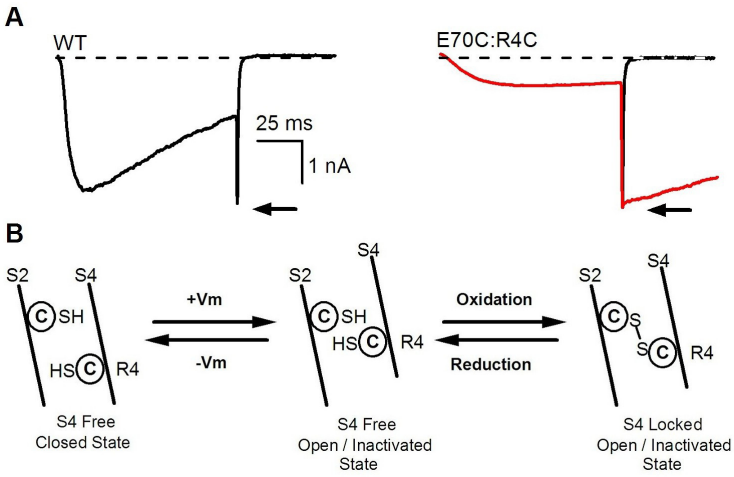

Fig. S2. Prevention of deactivation and engagement of inactivation by disulfide locking. (*A*) I_{Na} traces elicited by 100-ms depolarizations to 0 mV from cells expressing WT (black trace) and E70C:R4C (red trace) channels. For comparison, the WT tail current (black trace, *Right*) is superimposed on the E70:R4C recording. (*B*) Scheme representing the proposed state-dependent interaction of the cysteine residues upon activation and then inactivation.

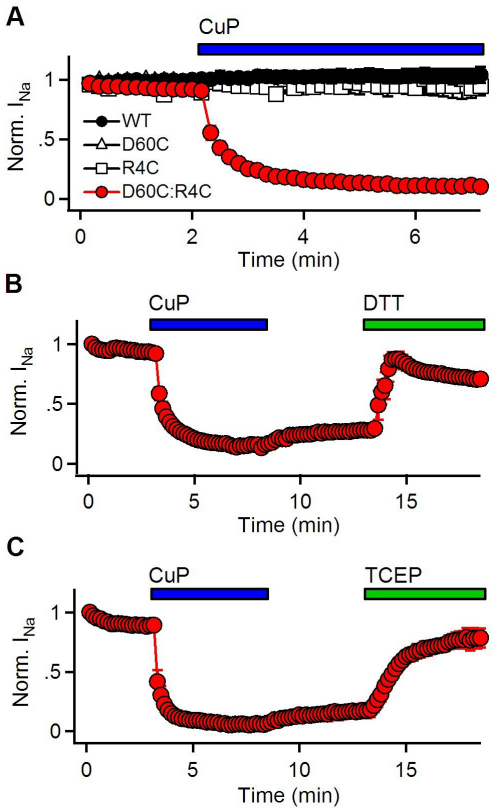

Fig. S3. D60C:R4C voltage-sensor disulfide locking by CuP. (*A*) Mean normalized peak I_{Na}^+ elicited by 0.1 Hz trains of 500-ms depolarizations to potentials equal to $V_{1/2}$ + 40 mV from a holding potential of −120 mV in tsA-201 cells expressing NaChBac WT, D60C, R4C, and D60C:R4C channels (n = 7). After 2 min in control saline, cells were exposed to the oxidizing agent CuP (100 μM CuP). (*B* and *C*) Mean normalized peak currents elicited by a 0.1 Hz train of 500-ms depolarizations to +80 mV from a holding potential of −120 mV in cells transfected with D60C:R4C channels (n = 8). After 3 min in control saline, cells were exposed to 100 μM CuP for 5 min. Then cells were washed with control saline for 5 min followed by a 5 min exposure to reducing agents 10 mM DTT (*B*) or 1 mM TCEP (*C*), as indicated

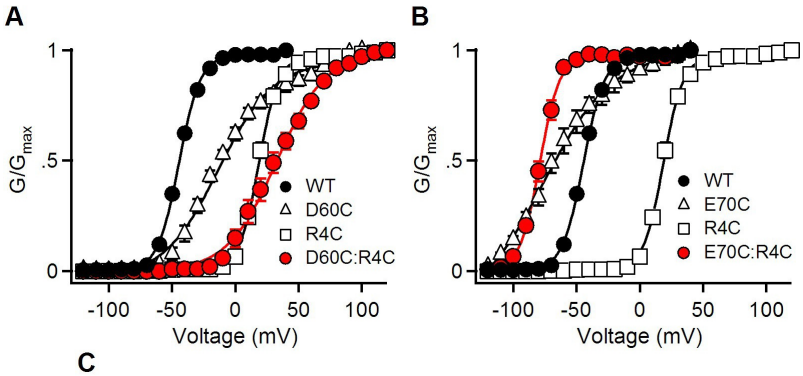

C

Channel	Z	$V_{1/2}$	ΔG°	ΔΔG°	ΣΔG°
WT	3.8 ±0.1	-43 ±2	-3.9 ±0.2	-	-
D60C	2.6 ±0.2	-19 ±3	-1.1 ±0.2	2.6	-
E70C	2.3 ±0.1	-72 ±3	-3.8 ±0.2	-0.1	-
R4C	4.2 ±0.1	15 ±2	1.5 ±0.2	5.2	-
D60C:R4C	2.9 ±0.1	36 ±3	2.4 ±0.2	6.2	-1.7
E70C:R4C	3.7 ±0.2	-79 ±2	-6.7 ±0.3	-3.0	-8.2

Fig. S4. Energy coupling of R4C with E70C and D60C. Conductance-voltage (G-V) relationships are plotted for (*A*) WT, D60C, R4C, and D60C:R4C channels and (*B*) WT, E70C, R4C, and E70C:R4C channels. Conductance-voltage relationships were calculated from peak I_{Na} elicited by 100-ms depolarizations to the indicated potentials ($n = 10$; ±SEM) as described in *Methods*. (*C*) Mutant cycle analysis. From the measured G-V relationships for the WT and mutant NaChBac channels, values for Z and $V_{1/2}$ in mV are tabulated. $\Delta G° = ZV_{1/2}*0.02306$, the free energy (kcal/mol) required to shift the channel from the closed to open state at 0 mV. ΔΔG° (kcal/mol) is the perturbation free energy of the mutant channel relative to the wild-type. ΣΔG ° is the nonadditive free energy or free energy coupling; the difference between the sum of the perturbation free energy of a double-mutant channel containing both mutations and the perturbation-free energies of the single-mutant channels. Equations used for these calculations are described in *SI Methods*.

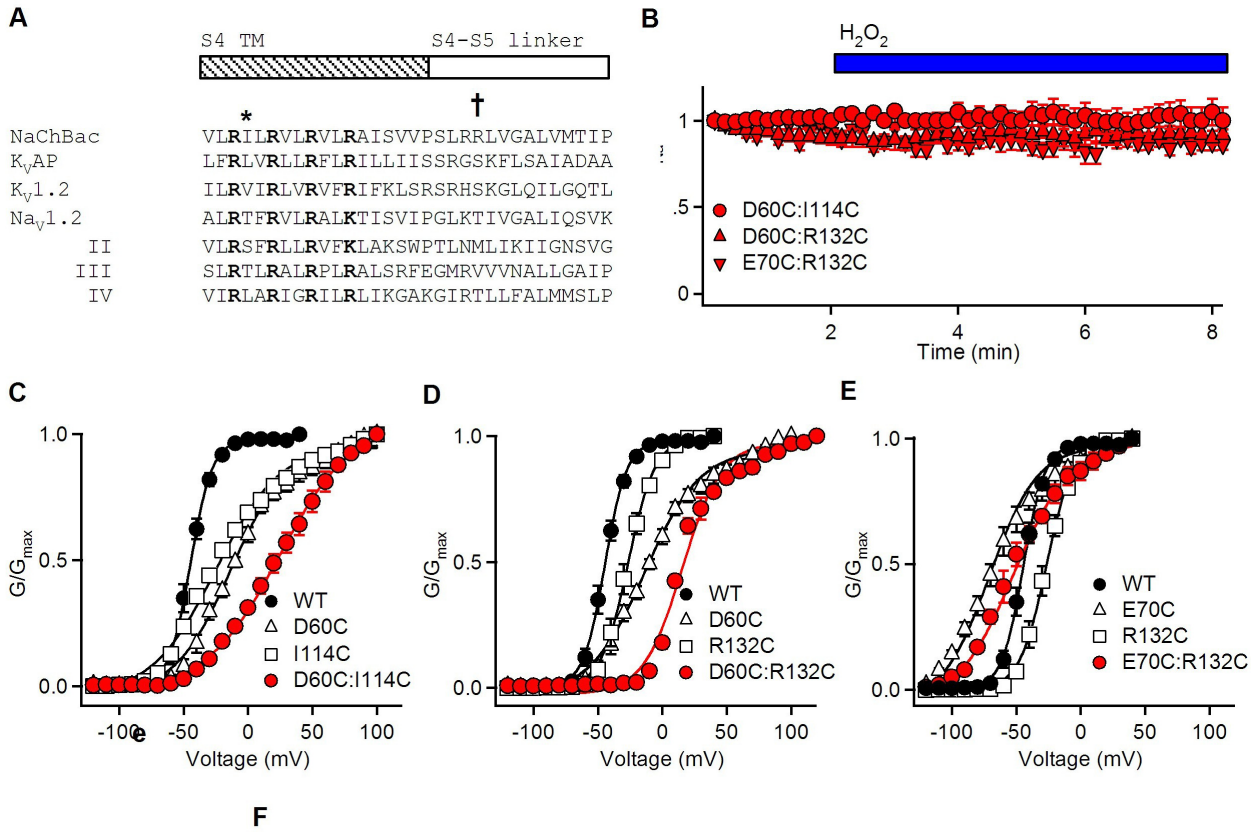

F

Channel	Z	$V_{1/2}$	ΔG°	ΔΔG°	ΣΔG°
WT	3.8 ±0.1	-43 ±2	-3.8 ±0.2	-	-
D60C	2.6 ±0.2	-19 ±3	-1.1 ±0.2	2.6	-
E70C	2.3 ±0.2	-72 ±3	-3.8 ±0.2	-0.1	-
I114C	2.8 ±0.2	-30 ±2	-1.9 ±0.2	1.9	-
R132C	3.1 ±0.2	-31 ±2	-2.2 ±0.2	1.6	-
D60C:I114C	1.9 ±0.2	18 ±2	0.7 ±0.2	4.5	0.1
D60C:R132C	2.7 ±0.2	11 ±2	0.7 ±0.2	4.5	0.3
E70C:R132C	2.0 ±0.2	-53 ±3	-2.4 ±0.2	1.3	-0.2

Fig. S5. Lack of disulfide locking and energy coupling of R132C and I114C. (*A*) Alignment of the amino acids of S4–S5 linkers of NaChBac, K_VAP, K_V1.2, and the four domains of Na_V1.2. The position of R132 in NaChBac is indicted by a dagger and I114 by an asterisk. (*B*) Mean normalized peak I_{Na}^+ elicited by 0.1 Hz trains of 500-ms depolarizations to $V_{1/2}$ + 40 mV from a holding potential of −120 mV in cells expressing NaChBac D60C:I114C; D60C:R132C and E70C:R132C channels (n = 5). After 2 min in control saline, cells were exposed 10 mM H_2O_2 for 6 min. Conductance-voltage relationships are plotted for (*C*) WT, I114C, D60C, and D60C:I114C; (*D*) WT, D60C, R132C, and D60C:R132C channels; and (*E*) WT, E70C, R132C, and E70C:R132C channels calculated from I_{Na} elicited by 100-ms depolarizations to the indicated potentials (n = 10; ± SEM). (*E*) Mutant cycle analysis. Values of ΔG°, ΔΔG°, and ΣΔG° calculated as described in the legend to Fig. S4.